DOI: 10.1002/cmdc.200900146

Elastic Potential Grids: Accurate and Efficient Representation of Intermolecular Interactions for Fully Flexible Docking

Sina Kazemi,[a] Dennis M. Krüger,[a] Finton Sirockin,[b] and Holger Gohlke*[a]

Protein–ligand docking is the major workhorse in computer-aided structure-based lead finding and optimization.[1,2] Predicted protein–ligand complex configurations are used for studying protein–ligand interactions, estimating binding affinities, and as a final filter step in virtual screening.[3] Early methods on protein–ligand docking treated either both proteins and ligands as rigid molecules[4] or allowed for conformational flexibility of only the ligand,[5–7] following a "rigid receptor hypothesis".[8] However, pronounced plasticity upon ligand binding has been observed for several pharmacologically important proteins, such as HIV-1 protease,[9–13] aldose reductase,[14–16] FK506 binding protein,[17–19] renin,[20–22] and dihydrofolate reductase (DHFR).[23–26] Protein plasticity comprises a range of possible movements, from single side chains to drastic structural rearrangements as seen in calmodulin.[27] Not surprisingly, if docking is performed with the assumption of a rigid active site in those cases, a dramatic decrease in docking accuracy is observed:[28,29] Whereas a docking success rate of 76% was reported for docking a ligand back to the protein structure derived from the ligand's co-crystal structure ("re-docking"), this rate dropped to only 49% if the ligands were docked against protein structures derived from other ligands' co-crystal structures ("cross docking").[29] Similar drop-offs have also been reported by others.[30,31] Furthermore, the drop in docking accuracy was found to be mirrored by the degree to which the protein moves upon ligand binding[30,32] so that docking to an empty form ("apo docking") usually shows the largest deterioration.[28] This clearly highlights the importance of developing strategies for taking protein plasticity into account in addition to the conformational flexibility of the ligand (henceforth referred to as "fully flexible docking") to prevent mis-dockings of ligands to flexible proteins.

At present, three major routes to include protein plasticity during docking can be identified. The classification correlates with various types of protein movements observed upon ligand binding. First, plasticity is considered implicitly following a soft-docking strategy with attenuated repulsive forces between protein and ligand.[33,34] While this is simple to implement and does not compromise docking efficiency, the range of possible movements that can be covered is rather limited. Second, only side chain conformational changes in the binding pocket are modeled.[35–40] These approaches assume that the protein has a rigid backbone structure, thus neglecting critical backbone shifts responsible for mis-docking of ligands.[29] Third, large-scale conformational changes including backbone motions are taken into account. There are several types of approaches in this category: perform parallel docking into multiple protein conformations;[31,41,42] structurally combine multiple conformations;[43–45] model protein motions in reduced coordinates;[46–48] apply molecular dynamics or Monte Carlo based sampling to either generate protein–ligand configurations[19,49,50] or optimize pre-computed configurations.[51]

Docking accuracy and computational efficiency determine the scope and quality of a docking approach. As for the first, fully flexible docking should ultimately become as accurate as "re-docking" pursued with a "rigid receptor hypothesis". Preserving computational efficiency is equally important, given the short timeframe usually available for a docking run. In particular, evaluating the interaction energy between protein and ligand is expensive. A widely used approach to increase the calculation speed is based on potential fields that are pre-calculated just once in the binding pocket region of the protein, by scanning interactions between the protein and ligand atom probes.[4,52–55] The potential field values are stored at the intersections of a *regular* 3D grid, providing a lookup table. The approach is applicable to all distance-dependent pairwise interactions, such as electrostatic and van der Waals interactions[4] and interactions described by statistical pair potentials.[3] In subsequent docking runs, interaction energies between protein and ligand are then determined in constant time from the lookup table by means of interpolation. This provides a significant rate increase relative to individually evaluating the pair interactions. However, this *regular* 3D grid-based approach is incompatible with fully flexible docking, because the lookup table values would need to be recalculated for every new protein conformation considered.

In the present study, we therefore developed an accurate representation of intermolecular interactions that makes use of the high efficiency in evaluating protein–ligand interaction energies from lookup tables even in the case of a moving protein. The new lookup table function for potential fields that we introduce is based on *irregular*, *deformable* 3D grids (Figure 1). The underlying idea is to adapt a 3D grid with pre-calculated potential field values, which were derived from an initial protein conformation, to another conformation by moving intersection points in space, but keeping the potential field values constant. As in the case of a regular 3D grid, interaction energies between ligand and protein are then determined from this lookup table. In contrast to the established approach, however, new protein conformations can now be sampled

[a] S. Kazemi, D. M. Krüger, Prof. Dr. H. Gohlke
Institut für Pharmazeutische und Medizinische Chemie
Heinrich-Heine-Universität
Universitätsstr. 1, 40225 Düsseldorf (Germany)
Fax: (+49) 211-81-13847
E-mail: gohlke@uni-duesseldorf.de

[b] Dr. F. Sirockin
Novartis Pharma AG, 4002 Basel (Switzerland)

Supporting information for this article is available on the WWW under http://dx.doi.org/10.1002/cmdc.200900146.

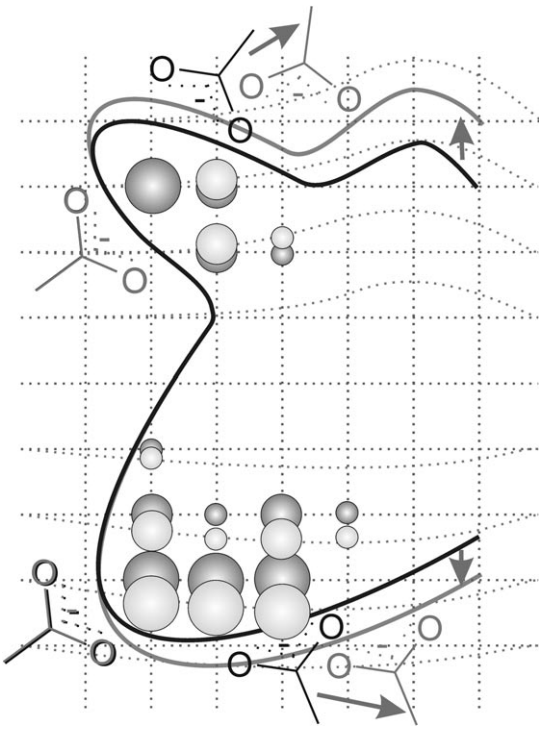

Figure 1. Schematic view of the spatial deformation of potential fields inside a binding pocket according to movements of the surrounding protein. Note that potential field values remain constant, as indicated by the size of moving spheres.

during a docking run without the need to recalculate potential field values.

Two requirements must be met for this approach to be successful. First, a method needs to be established that translates movements of the protein into appropriate displacements of the grid intersection points in the binding pocket region. Second, an efficient interpolation scheme is needed to determine protein–ligand interactions from the irregular, deformed 3D grid during a docking run (see below). With regard to the first, we propose to model the irregular, deformable 3D grid as a *homogeneous linear elastic body* (see also Supporting Information). Using elasticity theory[56,57] solutions to problems that describe the distribution of stress (or strain or displacement) in an elastic body under prescribed outer forces can be obtained. Most interesting for us is the relation between the displacement $\vec{u}$ of a point in the body (in our case, a grid intersection point) and forces $\vec{F}$ exerted at some other regions (in our case, due to protein movements). The relation between $\vec{u}$ and $\vec{F}$ is governed by Navier's equation [Eq. (1)]:

$$G\Delta\vec{u} + (\lambda + G)\nabla Div\,\vec{u} + \vec{F} = 0 \qquad (1)$$

in which ∇ is the Nabla operator, Δ is the Laplace operator, and *Div* is the divergence operator. The modulus of rigidity G and Lamé's constant λ are parameters that determine the elastic properties of the body. By coupling protein atoms to nearby grid intersection points by means of harmonic springs, protein atom movements $\vec{d}$ give rise to the elastic body-deforming forces $\vec{F} = k \cdot \vec{d}$, with k being the force constant. As in the general case no analytical solution can be found for Equation (1), we solve it by finite difference techniques.[58]

Our model for translating protein movements into grid intersection displacements contains three adjustable parameters. To determine reasonable and general values for G, λ, and k, we performed a training procedure based on an evolutionary algorithm (see also Supporting Information). During the training procedure, a regular 3D grid with potential field values calculated for a starting protein conformation was deformed according to experimentally determined protein movements following Equation (1). As an objective function, we required that the atomic environment of a grid intersection point remains preserved, i.e., the sum of squared deviations between grid intersection point-atom distances becomes minimal when compared between the starting and the deformed grids. This is based on the reasoning that if the grid intersection point-atom distance pattern remains the same during a deformation, potential field values will not change either. For the training, we used 36 protein–ligand complex structures with mandelate racemase, ricin, trypsin, and p38 MAP kinase as receptors (Supporting Information table S1). These structures served in previous evaluations of fully flexible docking approaches[31,37,41,43,59] and represent a range of protein movements: in addition to side chain movements in the case of trypsin[43,60] and ricin,[37,43,61] backbone and loop motions are observed in mandelate racemase[43,62] and p38 MAP kinase.[63,64] Notably, none of these targets have been used for evaluating our approach in docking later on, thus guaranteeing the training and evaluation procedures to be disjunct.

In initial training runs, values close to zero were obtained for λ. This is not unexpected, because λ is linked to Poisson's ratio,[56] which describes the expansion or contraction of an elastic body perpendicular to an applied force. We thus decided to set $\lambda = 0$ for subsequent training runs, not allowing any transverse strain in the elastic body. This leaves us with the ratio k/G as the only parameter that still needs to be determined for Equation (1). For 72 deformations of the 3D grid according to experimentally determined protein movements across the four different target classes, the ratio k/G was found to be 30.00 ± 0.24 (Supporting Information figure S3). This result is encouraging because it demonstrates that the parameterization of our approach is transferable between different complex classes, irrespective of the kinds of conformational changes observed.

The interpolation scheme for determining protein–ligand interactions from the 3D grid requires that for a given point in space, neighboring grid intersection points are identified, which then serve as data points for the interpolation. We apply an efficient hashing technique for this. For the hash map, the space encompassing the 3D grid is divided into cubes, with each of the cubes linked to a list of grid intersection points contained in it. During interpolation, cubes in the neighborhood of a given point in space are first identified. Subsequently, neighboring intersection points of the irregular 3D grid are looked up from the cube lists, resulting in a constant time complexity on average, as in the case of a regular

3D grid. When testing this approach on more than 100 randomly deformed 3D grids of a typical size used during docking ($61\times61\times61$), still one half of the number of interpolations per unit time can be achieved relative to the AutoDock trilinear interpolation function for a regular 3D grid.

Docking into deformable potential grids was evaluated using a modified version of AutoDock 4.1.6[52,65] as docking engine and the distance-dependent pair-potentials of DrugScore[66] as scoring function. This combination has already proven reliable in a "re-docking" evaluation.[3] The evaluation was performed on five different datasets of protein–ligand complexes with pharmaceutical relevance (aldose reductase, cAMP-dependent protein kinase, cyclin-dependent kinase 2, HIV-1 protease, and lymphocyte-specific kinase). The datasets were recently used in other fully flexible protein–ligand docking studies as well.[31,43,44] The datasets include between 4 and 20 holo structures and one apo structure, respectively. The following criteria were applied for choosing the datasets: 1) All target proteins are characterized by pronounced but distinct movements upon binding; aldose reductase shows large but localized side chain movements within the binding site, e.g., a flip of Leu300. In contrast, HIV-1 protease reveals a large and collective conformational change of the flap regions. In the case of the kinases, coupled backbone and side chain movements in flexible loop regions essentially influence the molecular recognition properties of the binding sites, and hence the binding modes of ligands. 2) Docking the ligands back into the bound receptor structures ("re-docking") was successful in all cases, with success rates between 42% for CDK2 and 100% for CAPK (Table 1). In contrast, docking to the apo structures largely failed (success rates between 5 and 29%; Table 1), with the largest drop in docking accuracy observed for HIV-1 protease. The "re-docking" results thus illustrate that the combination of docking engine and scoring function used here is appropriate, whereas it is the conformational changes of the proteins that diminish the success rate in the case of "apo docking".

Table 1. Success rates for re-docking, apo docking, and docking into deformed potential grids.[a]

	AR (5)	CAPK (7)	CDK2 (12)	HIV-1 Protease (20)	LCK (4)
Re-docking	3	7	5	19	3
Apo docking	1	2	2	1	1
Deformed grids	1	7	8	16	3

[a] The number of complexes is given for which a ligand configuration with $\leq$2 Å rmsd from the native structure was found as structure on the first rank of the largest cluster of docking solutions. The number of complexes used is given in parentheses.

We now evaluate the performance for docking into deformed potential grids. DrugScore potential values on the grids were initially calculated based on the apo protein structure. The grids were then deformed according to Equation (1), following protein movements from the apo to a holo conformation. As a result, the pre-calculated potential values from the apo binding site are shifted to new locations in the holo binding site. If the shifting is successful, we expect docking to the deformed grids to be as accurate as "re-docking" into the holo structure. Convincingly, this is indeed true for all datasets except that of aldose reductase: the success rates amount to 100% for CAPK, 67% for CDK2, 80% for HIV-1 protease, and 75% for LCK (Table 1). In the following, we analyze these docking successes and failures in greater detail.

An example of successful docking into deformed potential grids is depicted in Figure 2. Here, the conformational change of the flap region of HIV-1 protease results in a collective movement involving the protein backbone and side chains.

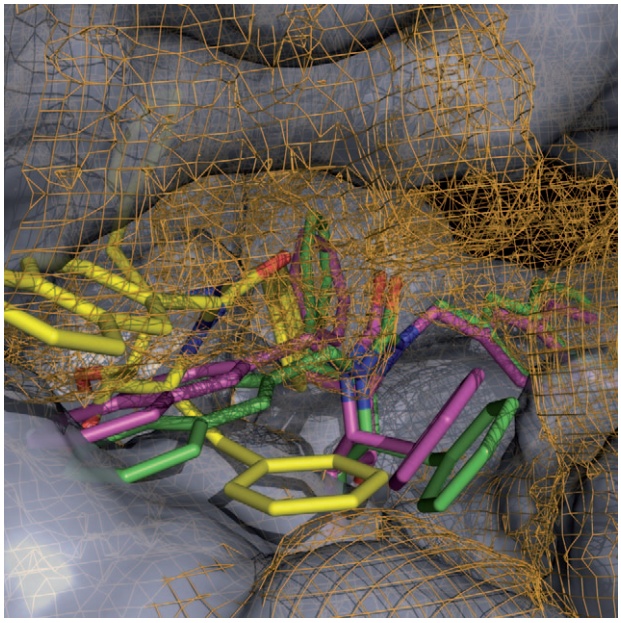

Figure 2. Docking of ligand XK263 into potential fields generated from an HIV-1 protease apo structure (PDB code: 3HVP), but deformed to the holo structure 1HVR. The repulsive potential fields for aromatic carbon of 3HVP are depicted in blue, whereas the deformed fields are depicted in orange. Carbon atoms of the ligand are displayed in green for the native ligand pose of 1HVR, yellow for the apo docking solution, and magenta for the solution found for docking into the deformed grids (rmsd to the native structure: 0.65 Å), respectively. The image was prepared using PyMOL version 0.99rc6.

Without taking into account these conformational changes, the binding pocket of the apo structure (PDB code: 3HVP) is too wide, so that a docking solution for the ligand XK263 (PDB code: 1HVR) is found that deviates by 4.34 Å from the experimental one. In turn, if the protein movements are mimicked by the grid deformation, the binding pocket is narrowed, and the configurational space accessible to the ligand is limited. Docking into the deformed grids results in a ligand pose that only deviates by 0.65 Å rmsd from the native structure. An analysis of the binding energy landscape (see Supporting Information figure S4) in this case reveals that the deformed potential grids provide a well-behaved representation of protein–ligand interactions, as they produce a binding energy land-

scape that is smooth and has a funnel shape similar to the landscape of the holo structure. In contrast, the apo structure results in a landscape without any funnel shape, but a global minimum between 4 and 5 Å rmsd from the native structure, in agreement with the finding that docking was unsuccessful in this case.

Another case of successful docking into deformed grids is depicted in Figure 3. Previous studies have already stressed the need to consider receptor movements of CAPK in addition to ligand flexibility during docking.[31,67] For docking staurosporine, combined backbone and side chain motions must be modeled, in particular in the C-terminal loop containing Phe 327. Figure 3 shows that the protein movements upon ligand binding are very well accommodated by the deformed potential grids, which were again generated from the apo structure of CAPK (PDB code: 1JLU) and deformed toward the bound structure (PDB code: 1STC). The movement of Phe 327 in particular "drags along" the attractive field for aromatic carbon, which eventually allows docking of staurosporine with 0.64 Å rmsd to the native structure.

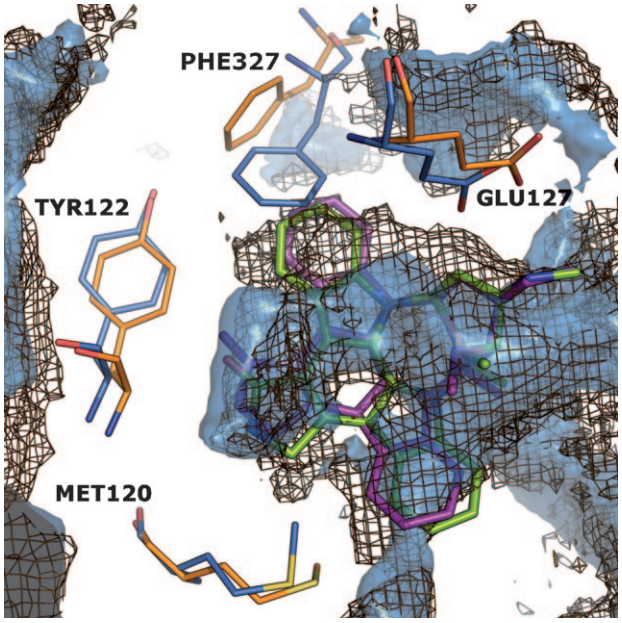

Figure 3. Docking of staurosporine into potential fields generated from the CAPK apo structure (PDB code: 1JLU), but deformed to the holo structure 1STC. The attractive potential fields for aromatic carbon and side chain conformations of 1JLU are depicted in blue. Deformed potential fields and side chain conformations of 1STC are depicted in orange. Aside from side chain movements, backbone motion can also be observed. Staurosporine carbon atoms are displayed in green for the native structure and magenta for the solution found for docking into the deformed grids (rmsd to the native structure: 0.64 Å). Note how the most significant movement of Phe 327 "drags along" the potential field.

The above data demonstrate, as a proof-of-principle, that if the protein movement is known, docking into deformed potential grids is generally as successful and efficient as docking into the respective holo structure. We note that the potential grids were generated from the apo structure, and "apo docking" is usually considered to be more difficult than docking to another holo structure or an average structure of the target.[28] This is a remarkable result because it shifts the challenge of algorithmic development in the field of fully flexible docking toward generating appropriate protein movements. Several alternatives are already available for this: protein conformations have been successfully generated by MD simulations[19,49,50] or based on normal modes or reduced coordinates from elastic network models.[46–48]

In the latter case, it is interesting to note that the theory of linear elasticity then serves as a consistent model throughout: it underlies the modeling of the protein movement, the protein atom-grid intersection coupling by harmonic springs, and the deformation of the potential grids. As a further advantage of the linear regime of elasticity, two or more strain fields acting on an elastic body may be combined by direct superposition, and the order of application of these fields has no effect on the final deformation of the body.[56,57] This implies that grid deformations due to protein motions along linear combinations of normal mode directions can be obtained efficiently by adding displacement vectors of grid intersection points that resulted from solving Equation (1) for each normal mode motion separately. Finally, the theory of linear elasticity requires that the displacements of grid intersection points are small relative to the dimensions of the grid.[56] Figure S5 (Supporting Information) demonstrates that even for protein movements above 2 Å rmsd, convincing improvements in the predicted ligand configurations can be achieved when using elastic potential grids. We thus expect our approach to have a sufficiently broad range of applicability.

Perhaps more important than the *magnitude* of motion is the *type* of motion that can be considered. On the one hand, we note that our approach does allow consideration of side chain and backbone motions simultaneously, which is important in light of the findings that backbone conformational changes of even 1 Å can significantly affect receptor–ligand interactions.[68] On the other hand, limitations of the approach become clear in the case of the aldose reductase dataset. Here, Leu 300 undergoes a rotational flip motion, which leads to a large local conformational change that cannot be treated adequately by our approach (Supporting Information figure S6). Consequently, no improvement for the docking into deformed grids relative to docking to the apo structure is observed (Table 1). Likewise, we expect our approach to fail in the case of 180° rotations of the amide groups of Asn and Gln. The exchange of a hydrogen bond donor interaction with an acceptor interaction cannot be modeled by elastic deformation of the potential grids: although grid intersection points can change their location, the grid topology (i.e., the ordering of grid intersection points) cannot be changed. Excising grid regions close to protein parts that show rotational movements and carrying along those regions as such with the moving part may provide a satisfying solution in these cases.

As for the general scope of our approach, conformational adaptation of binding partners upon complex formation is not limited to the field of protein–ligand complexes, but occurs in the case of RNA–ligand and macromolecule–macromolecule

complexes, too. At present, we see no reason why our approach could not be transferred to docking involving these complexes.

Acknowledgements

We are grateful for financial support by Novartis Pharma AG, Basel. We thank Domingo Gonzalez Ruiz for critically reading the manuscript.

Keywords: docking methods · drug design · molecular recognition · protein flexibility · protein–ligand complexes

[1] B. K. Shoichet, S. L. McGovern, B. Wei, J. J. Irwin, *Curr. Opin. Chem. Biol.* **2002**, *6*, 439.
[2] W. L. Jorgensen, *Science* **2004**, *303*, 1813.
[3] C. A. Sotriffer, H. Gohlke, G. Klebe, *J. Med. Chem.* **2002**, *45*, 1967.
[4] I. D. Kuntz, J. M. Blaney, S. J. Oatley, R. Langridge, T. E. Ferrin, *J. Mol. Biol.* **1982**, *161*, 269.
[5] M. Rarey, B. Kramer, T. Lengauer, G. Klebe, *J. Mol. Biol.* **1996**, *261*, 470.
[6] G. Jones, P. Willett, R. C. Glen, A. R. Leach, R. Taylor, *J. Mol. Biol.* **1997**, *267*, 727.
[7] B. K. Shoichet, I. D. Kuntz, *Chem. Biol.* **1996**, *3*, 151.
[8] A. M. Davis, S. J. Teague, G. J. Kleywegt, *Angew. Chem.* **2003**, *115*, 2822; *Angew. Chem. Int. Ed.* **2003**, *42*, 2718.
[9] H. Heaslet, R. Rosenfeld, M. Giffin, Y. C. Lin, K. Tam, B. E. Torbett, J. H. Elder, D. E. McRee, C. D. Stout, *Acta Crystallogr. Sect. D* **2007**, *63*, 866.
[10] V. Hornak, C. Simmerling, *Drug Discovery Today* **2007**, *12*, 132.
[11] R. Ishima, D. I. Freedberg, Y. X. Wang, J. M. Louis, D. A. Torchia, *Structure* **1999**, *7*, 1047.
[12] M. Kumar, M. V. Hosur, *Eur. J. Biochem.* **2003**, *270*, 1231.
[13] L. K. Nicholson, T. Yamazaki, D. A. Torchia, S. Grzesiek, A. Bax, S. J. Stahl, J. D. Kaufman, P. T. Wingfield, P. Y. Lam, P. K. Jadhav et al., *Nat. Struct. Biol.* **1995**, *2*, 274.
[14] J. M. Brownlee, E. Carlson, A. C. Milne, E. Pape, D. H. Harrison, *Bioorg. Chem.* **2006**, *34*, 424.
[15] C. A. Sotriffer, O. Kramer, G. Klebe, *Proteins* **2004**, *56*, 52.
[16] A. Urzhumtsev, F. Tete-Favier, A. Mitschler, J. Barbanton, P. Barth, L. Urzhumtseva, J. F. Biellmann, A. Podjarny, D. Moras, *Structure* **1997**, *5*, 601.
[17] J. W. Cheng, C. A. Lepre, J. M. Moore, *Biochemistry* **1994**, *33*, 4093.
[18] A. May, M. Zacharias, *Biochim. Biophys. Acta Proteins Proteomics* **2005**, *1754*, 225.
[19] M. Zacharias, *Proteins* **2004**, *54*, 759.
[20] M. Benkoulouche, M. Cotrait, B. Maigret, *J. Comput.-Aided Mol. Des.* **1992**, *6*, 79.
[21] N. A. Powell, E. H. Clay, D. D. Holsworth, J. W. Bryant, M. J. Ryan, M. Jalaie, E. Zhang, J. J. Edmunds, *Bioorg. Med. Chem. Lett.* **2005**, *15*, 2371.
[22] S. Thaisrivongs, D. T. Pals, S. R. Turner, L. T. Kroll, *J. Med. Chem.* **1988**, *31*, 1369.
[23] A. L. Bowman, M. G. Lerner, H. A. Carlson, *J. Am. Chem. Soc.* **2007**, *129*, 3634.
[24] I. H. Choi, C. Kim, *Arch. Pharmacal Res.* **2002**, *25*, 807.
[25] V. Cody, A. Wojtczak, T. I. Kalman, J. H. Friesheim, R. L. Blakley, *Adv. Exp. Med. Biol.* **1993**, *338*, 481.
[26] J. R. Schnell, H. J. Dyson, P. E. Wright, *Biochemistry* **2004**, *43*, 374.
[27] D. Barnard, B. Diaz, L. Hettich, E. Chuang, X. F. Zhang, J. Avruch, M. Marshall, *Oncogene* **1995**, *10*, 1283.
[28] J. A. Erickson, M. Jalaie, D. H. Robertson, R. A. Lewis, M. Vieth, *J. Med. Chem.* **2004**, *47*, 45.
[29] C. W. Murray, C. A. Baxter, A. D. Frenkel, *J. Comput.-Aided Mol. Des.* **1999**, *13*, 547.
[30] M. L. Verdonk, P. N. Mortenson, R. J. Hall, M. J. Hartshorn, C. W. Murray, *J. Chem. Inf. Model.* **2008**, *48*, 2214.
[31] C. N. Cavasotto, R. A. Abagyan, *J. Mol. Biol.* **2004**, *337*, 209.
[32] P. Ferrara, H. Gohlke, D. J. Price, G. Klebe, C. L. Brooks III, *J. Med. Chem.* **2004**, *47*, 3032.
[33] V. Schnecke, C. A. Swanson, E. D. Getzoff, J. A. Tainer, L. A. Kuhn, *Proteins* **1998**, *33*, 74.
[34] M. Y. Mizutani, Y. Takamatsu, T. Ichinose, K. Nakamura, A. Itai, *Proteins* **2006**, *63*, 878.
[35] T. M. Frimurer, G. H. Peters, L. F. Iversen, H. S. Andersen, N. P. Moller, O. H. Olsen, *Biophys. J.* **2003**, *84*, 2273.
[36] P. Källblad, P. M. Dean, *J. Mol. Biol.* **2003**, *326*, 1651.
[37] Y. Zhao, M. F. Sanner, *J. Comput.-Aided Mol. Des.* **2008**, *22*, 673.
[38] A. R. Leach, *J. Mol. Biol.* **1994**, *235*, 345.
[39] R. Najmanovich, J. Kuttner, V. Sobolev, M. Edelman, *Proteins* **2000**, *39*, 261.
[40] M. I. Zavodszky, L. A. Kuhn, *Protein Sci.* **2005**, *14*, 1104.
[41] S. Y. Huang, X. Zou, *Proteins* **2007**, *66*, 399.
[42] S. B. Nabuurs, M. Wagener, J. de Vlieg, *J. Med. Chem.* **2007**, *50*, 6507.
[43] H. Claussen, C. Buning, M. Rarey, T. Lengauer, *J. Mol. Biol.* **2001**, *308*, 377.
[44] F. Österberg, G. M. Morris, M. F. Sanner, A. J. Olson, D. S. Goodsell, *Proteins* **2002**, *46*, 34.
[45] R. M. Knegtel, I. D. Kuntz, C. M. Oshiro, *J. Mol. Biol.* **1997**, *266*, 424.
[46] C. N. Cavasotto, J. A. Kovacs, R. A. Abagyan, *J. Am. Chem. Soc.* **2005**, *127*, 9632.
[47] V. Tozzini, *Curr. Opin. Struct. Biol.* **2005**, *15*, 144.
[48] I. Bahar, A. J. Rader, *Curr. Opin. Struct. Biol.* **2005**, *15*, 586.
[49] M. Mangoni, D. Roccatano, A. Di Nola, *Proteins* **1999**, *35*, 153.
[50] R. Tatsumi, Y. Fukunishi, H. Nakamura, *J. Comput. Chem.* **2004**, *25*, 1995.
[51] N. Andrusier, R. Nussinov, H. J. Wolfson, *Proteins* **2007**, *69*, 139.
[52] D. S. Goodsell, A. J. Olson, *Proteins* **1990**, *8*, 195.
[53] R. Abagyan, M. Totrov, *J. Mol. Biol.* **1994**, *235*, 983.
[54] J. Y. Trosset, H. A. Scheraga, *Proc. Natl. Acad. Sci. USA* **1998**, *95*, 8011.
[55] R. A. Friesner, J. L. Banks, R. B. Murphy, T. A. Halgren, J. J. Klicic, D. T. Mainz, M. P. Repasky, E. H. Knoll, M. Shelley, J. K. Perry, D. E. Shaw, P. Francis, P. S. Shenkin, *J. Med. Chem.* **2004**, *47*, 1739.
[56] P. C. Chou, N. J. Pagano in *Elasticity—Tensor, Dyadic, and Engineering Approaches*, Dover, New York, **1992**.
[57] L. D. Landau, E. M. Lifshitz in *Theory of Elasticity*, Pergamon, London, **1959**.
[58] J. D. Faires, R. L. Burden, *Numerical Analysis*, PWS, Boston, **1998**.
[59] B. D. Bursulaya, M. Totrov, R. Abagyan, C. L. Brooks III, *J. Comput.-Aided Mol. Des.* **2003**, *17*, 755.
[60] E. Toyota, K. K. Ng, H. Sekizaki, K. Itoh, K. Tanizawa, M. N. James, *J. Mol. Biol.* **2001**, *305*, 471.
[61] B. J. Katzin, E. J. Collins, J. D. Robertus, *Proteins* **1991**, *10*, 251.
[62] J. R. Bourque, S. L. Bearne, *Biochemistry* **2008**, *47*, 566.
[63] C. E. Fitzgerald, S. B. Patel, J. W. Becker, P. M. Cameron, D. Zaller, V. B. Pikounis, S. J. O'Keefe, G. Scapin, *Nat. Struct. Biol.* **2003**, *10*, 764.
[64] S. R. Natarajan, S. T. Heller, K. Nam, S. B. Singh, G. Scapin, S. Patel, J. E. Thompson, C. E. Fitzgerald, S. J. O'Keefe, *Bioorg. Med. Chem. Lett.* **2006**, *16*, 5809.
[65] G. M. Morris, D. S. Goodsell, R. Huey, W. Lindstrom, W. E. Hart, S. Kurowski, S. Halliday, R. Belew, A. J. Olson, Molecular Graphics Laboratory, Department of Molecular Biology, The Scripps Research Institute, La Jolla, CA (USA), **2007**.
[66] H. Gohlke, M. Hendlich, G. Klebe, *J. Mol. Biol.* **2000**, *295*, 337.
[67] Y. Zhao, M. F. Sanner, *Proteins* **2007**, *68*, 726.
[68] A. May, F. Sieker, M. Zacharias, *J. Comput.-Aided Drug Des.* **2008**, *4*, 33.

Received: April 8, 2009
Revised: May 4, 2009
Published online on ■■ ■■, 2009

COMMUNICATIONS

*S. Kazemi, D. M. Krüger, F. Sirockin, H. Gohlke**

■■ – ■■

Elastic Potential Grids: Accurate and Efficient Representation of Intermolecular Interactions for Fully Flexible Docking

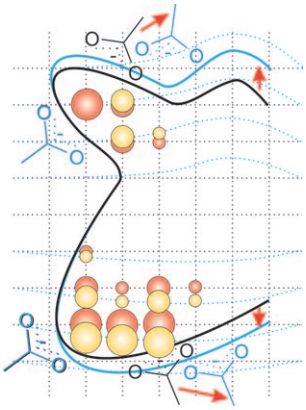

Potential fields represented by irregular, deformable 3D grids provide an accurate and efficient lookup table function for evaluating intermolecular interactions in docking algorithms that consider target flexibility. Target movements can be translated into appropriate displacements of grid intersection points in a binding site region if the irregular deformable 3D grid is modeled as a homogeneous linear elastic body.

